ISSN 1819-7140, Russian Journal of Pacific Geology, 2024, Vol. 18, No. 3, pp. 310–330. © Pleiades Publishing, Ltd., 2024.
Russian Text © The Author(s), 2024, published in Tikhookeanskaya Geologiya, 2024, Vol. 43, No. 3, pp. 88–108.

Geochemistry, Mineralogy, and Genetic Features of the Belogorskoe Magnetite Deposit (Sikhote-Alin)

V. T. Kazachenko[a], * and E. V. Perevoznikova[a], **

[a] *Far East Geological Institute, Far Eastern Branch, Russian Academy of Sciences, Vladivostok, Russia*

**e-mail: vkazachenko@mail.ru*

***e-mail: elenavalper@yandex.ru*

Received April 10, 2023; revised May 25, 2023; accepted January 11, 2024

Abstract—New data favor the view previously substantiated by geological, geochemical and isotopic data that the orebodies of the Belogorskoe deposit are the Triassic erosion products of the laterite weathering crust after gabbroids, which were metamorphosed and partially regenerated in the Late Cretaceous–Paleogene. The source for the formation of the Belogorskoe deposit was shown to be the products of exogenic destruction of rocks, the isotopic and geochemical characteristics of which are close to those of Cambrian gabbroids of the Vladimiro-Aleksandrovsky massif (southern part of the Okrainsko-Sergeevsky terrane). It has been found that the Belogorskoe deposit consists of rocks and ores, the primary (magmatic) REE distribution in which was variably modified as a result of interaction between sediments (protoliths) and seawater (presumably during the Late Jurassic–Early Cretaceous accretion), as well as between their metamorphosed analogues and hydrothermal solutions (in the Late Cretaceous–Paleogene). The influence of gabbroids (as a source of material) on the chemical and mineral composition of the Belogorskoe deposit agrees with the data reported in a paper on the enrichment of orebodies in such elements as Fe and Mn characteristic of ultramafic rocks and the presence of Au–Ag–Pd–Pt, Ni–Co, and Bi mineralization in them. The orebodies of the Belogorskoe deposit contain accessory minerals and mineral varieties that are rare in nature and poorly studied. They include an unusually Th-rich variety of zircon, baddeleyite, gudmundite, a large group of bismuth compounds, including Bi_2Te, $(Ag,Pb)BiS_2$, as well as coloradoite, lafossaite, sanbornite, perovskite, and the compound $InPO_4$. There is also a large group of rare and unusual noble metal compounds: copper gold, platinum gold, jonassonite, disordered solid solutions of Cu, Ag and Au (Au-based), Pt–Pd, Pt–Ag intermetallides, and other rare minerals and mineral varieties.

Keywords: magnetite deposit, metalliferous sediments, contact metamorphism, mineralogy, Sikhote-Alin

DOI: 10.1134/S1819714024700064

INTRODUCTION

Calc-silicate rocks with base-metal, boron, and iron ores are typical of South Sikhote-Alin. They are confined to fragments of Triassic and Devonian–Carboniferous reef massifs and have high Mn and Fe contents. Calc-silicate rocks have been previously attributed to skarns, but according to our published data, they represent Triassic metalliferous sediments that were contact-metamorphosed and partly regenerated in the Late Cretaceous–Paleogene. They are widespread in the well-studied Dalnegorsk borosilicate and base metal (Vtoroi Sovetsky, Nikolaevsky, Verkhnee, Sadovoe, Partizanskoe, etc.) deposits in the Dalnegorsk ore district [2, 16, 17, 19, 22]. Calc-silicate rocks with iron ores are present at the Belogorskoe, Pershinskoe, Mramorny Mys, and other deposits of the Olga ore district [3, 6, 7, 13].

Our previous studies were aimed at revealing the genetic features of calc-silicate rocks and associated base-metal, borosilicate, and iron ores. In particular, we obtained and published new data on rock-forming and accessory minerals (including the Au–Ag–Pd–Pt mineralization) in calc-silicate rocks of borosilicate and base-metal deposits. The rock-forming minerals and accessory noble metal and bismuth mineralization were studied in calc-silicate rocks of the Belogorskoe magnetite deposit [9].

The objective of this study was to obtain new data on the origin of calc-silicate rocks and magnetite mineralization of the Olga ore district by the example of the Belogorskoe deposit. This study analyzes and generalizes new and already published materials on this object. New data are reported on a large group of accessory minerals first discovered at the deposit. Their position in the mineral formation process is shown. Additional evidence is reported to substantiate the sedimentary nature of the deposit, and a new view is proposed on the problem of ore sources based on geochemical and isotope data.

REGIONAL POSITION AND GEOLOGICAL STRUCTURE OF THE DEPOSIT

The Belogorskoe deposit is located in the Olga ore district of the Taukha terrane (Fig. 1). The district (Fig. 2) is made up of Late Cretaceous–Paleogene volcanogenic rocks and granitoids of the Eastern Sikhote-Alin intrusive–volcanogenic belt, among which blocks and "erosion windows" of sedimentary and biogenic rocks are exposed. The eastern and northeastern parts of the area consist of granitoids of the Vladimirsky massif dated at 67.9 [18] or 64–71 Ma [30]. Rocks of sedimentary and biogenic origin are present as large blocks of reef limestones, deformed siliceous and siliceous–clayey schists with an age interval from Late Devonian to Late Carboniferous [11] and fragments of a Triassic chert formation embedded in a terrigenous matrix of the mélange complex of the Late Jurassic–Early Cretaceous accretionary wedge. All of them form a discontinuous band 4–9 km wide extending in the northeastern direction throughout the entire area. The Triassic chert formation contains jaspers, as well as silicate–magnetite ores, siliceous–rhodochrosite, manganese silicate (mainly Mn silicates), and spessartine–quartz rocks that formed owing to diagenesis and contact metamorphism of metalliferous sediments. They make up stratal and lenticular bodies from a few centimeters to a few meters thick and tens to a few hundreds of meters long on the surface, which form a unit or replace each other by strike. Sedimentary rocks are deformed into NE-trending asymmetrical folds complicated by thrusts and faults of other types.

The Belogorskoe deposit is confined to the contact between a block of Middle Carboniferous reef limestones [11] and the Vladimirsky granitoid massif. The contact is complicated by a sublongitudinal fault (associated with dacite bodies) (Fig. 3) and consists of the lenticular Margaritovskaya, Belogorskaya, Blagodatnaya, and Skal'naya orebodies. Basaltic, dioritic, and rhyolitic dikes supposedly of the Primorsky (Turonian–Santonian) intrusive complex are widespread over the deposit area.

The oldest (metamorphic) rocks of main orebodies (Blagodatnaya, Belogorskaya, and Margaritovskaya) are represented by massive garnet and banded garnet–magnetite rocks (with an insignificant amount of apatite, datolite, cuspidine, clinopyroxene, bustamite, and vesuvian). Garnet and garnet–magnetite rocks contain numerous small later calcite pockets, systems of thin winding veinlets and thin short veins of calcite (sometimes with fluorite, rhodonite, and relict garnet) composition, whose accumulation sites contain almost monomineralic blocks of massive magnetite with vague boundaries [9]. The blocks are associated with pockets (up to 1 m and more across) of coarse-crystalline calcite. They contain subordinate amount of coarse-crystalline fluorite, as well as sphalerite with short veins (up to 1 cm thick or more) confined to the cleavage planes of carbonate and fluorite, thus forming a lattice. Near these pockets, garnet and garnet–magnetite rocks contain amphibole–rhodonite segregations (up to few tens of centimeters in size).

METHODS

Lump samples were collected for analytical studies. The Mn, P, and Zn contents were determined by atomic emission spectrometry with inductively coupled plasma on an ICAP 6500Duo (Thermo Electron Corporation, USA) spectrometer at the Laboratory of Analytical Chemistry of the Far East Geological Institute, Far Eastern Branch, Russian Academy of Sciences. Trace elements were analyzed there by the inductively coupled plasma mass spectrometry on an Agilent 7500 c spectrometer (Agilent Technologies, USA). Samples were prepared for analysis by fusion with lithium metaborate. The inner standards were In and Bi at final concentration of 10 ppb in solution. The accuracy of analyses was controlled by the measurement of rock standards: JG-3, JB-3, JA-2 of the Geological Survey of Japan and Russian Standards SG-3 (GSO No. 3333-85), ST-2 A (GSO No.8671-2005). The relative mean-square deviations for most elements are no more than 5–15%, which corresponds to the quality criteria of element analysis accepted in geochemical studies. The detection limits were as follows (ppm): La, Ce—0.01; Pr, Sm, Eu, Tb, Er, Yb, Lu—0.002; Nd—0.005; Gd, Ho, Tm—0.003; Dy—0.001; Cr—0.9; Co—0.03; Ni, Zn—0.3; Cu—0.1.

Sample preparation and the measurements of Nd isotopic composition for rocks were carried out at the Geological Institute of the Kola Science Center of the Russian Academy of Sciences. The analyses were prepared on a seven-channel solid-phase Finnigan-MAT 262 (RPQ) spectrometer operating in a double Re and Ta filament mode. The mean $^{143}Nd/^{144}Nd$ ratio in the La Jolla standard during the measurements was 0.511835 ± 18 ($N = 15$). The precision of Nd isotope measurement in a single analysis was no higher than 0.004%. The laboratory blank was 0.3 ng Nd, while the measurement accuracy was ±0.5%. The isotope ratios were normalized to $^{146}Nd/^{144}Nd = 0.7219$ and then adjusted to $^{143}Nd/^{144}Nd = 0.511860$ in the La Jolla standard.

The identification of minerals was carried out under microscope in transmitted and reflected light and confirmed by their microprobe analysis. The minerals were analyzed in polished sections at the Far East Geological Institute of the Far Eastern Branch of the Russian Academy of Sciences using a JXA8100 microprobe equipped with tree wavelength spectrometers and EDS INCAx-sight energy dispersive spectrometer at an accelerating voltage of 20 kV and beam current of 1×10^{-8} A. The contents of all elements were determined using EDS. The radiation sampling angle was 45° and the locality of the analysis was 1 μm. Quanti-

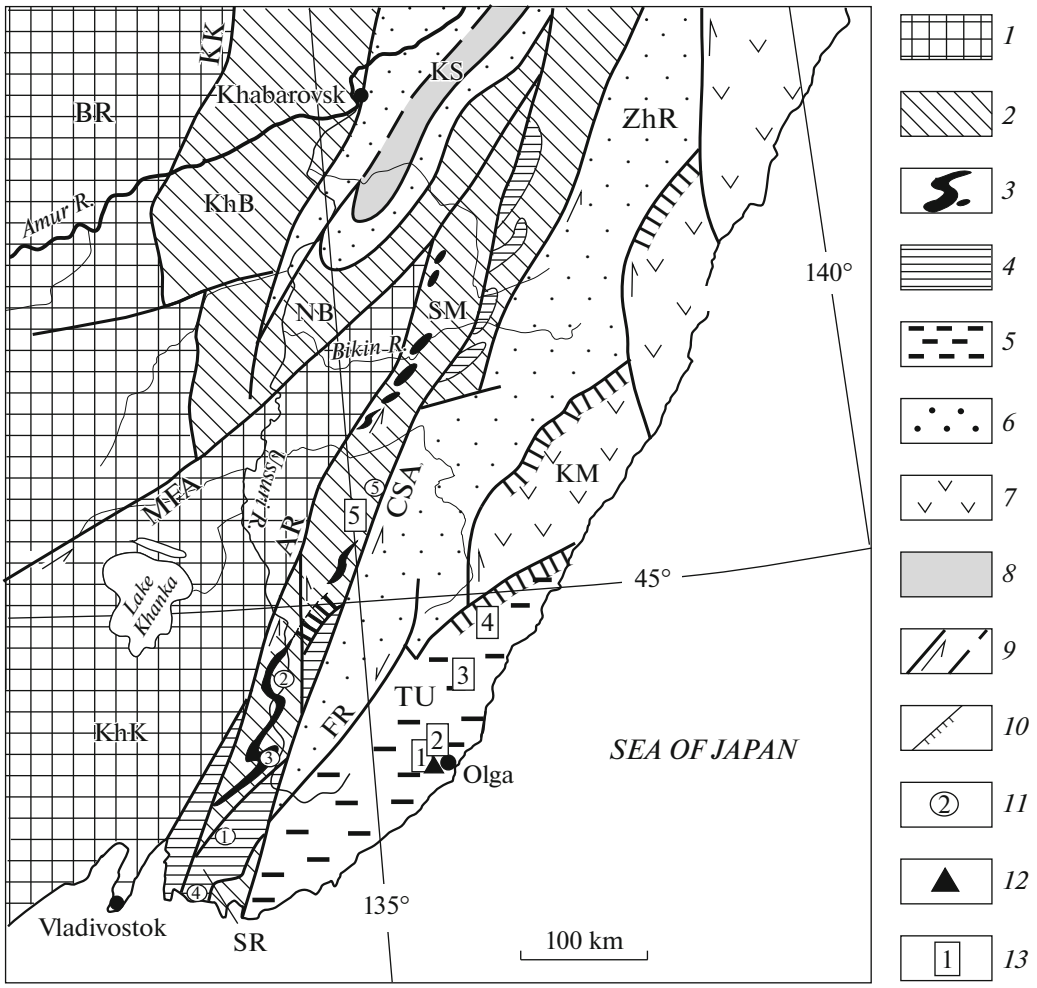

Fig. 1. Location of studied objects in Sikhote-Alin; tectonic basis modified after A.I. Khanchuk [4]. (*1*) (KhN) Khanka massif, (BR) Bureya massif; (*2*) Jurassic terranes (fragments of accretionary wedges): (KhB) Khabarovsk, (SM) Samarka, (NB) Nadankhada–Bikin, (*3*) Kalinovsky gabbroids (Devonian?); (*4*) Okrainsko–Sergeevsky terrane (SR) and its fragments (gabbroids of Sergeevsky complex and other rocks), which were involved in structures of Jurassic accretionary wedge and experienced a cycle of syn- and postaccretionary transformations; (*5*, *6*) Early Cretaceous terranes—fragments: (*5*) Neocomian accretionary wedge (TU) Taukha; (*6*) near-continental pull-apart turbidite basin ((ZR) Zhuravlevka–Amur); (*7*) Barremian–Albian island arc system ((KM) Kema); (*8*) Albian accretionary wedge ((KS) Kiselevka–Manoma); (*9*) sinistral strike-slips, including: (KK) Kukan, (AR) Arsen'evsky, (MFA) Mishan–Fushun (Alchan), (CSA) Central Sikhote-Alin, and (FR) Furman; (*10*) overthrust; (*11*) sampling localities: (1) around village of Sergeevka (rocks of Sergeevsky and Avdokimovsky complexes), (2) near village of Kamenka (Sergeevsky and Avdokimovsky complexes), (3) in vicinity of Verkhnyaya Breevka village (Breevsky quarry, Kalinovsky Complex), (4) near village of Vladimiro–Aleksandrovsky (Vladimiro–Aleksandrovsky massif), (5) near village of Dalny Kut (Dalny Kut massif); (*12*) Belogorskoe deposit; (*13*) studied areas with exposures of contact-metamorphosed Triassic metalliferous sediments: (1) Shirokaya pad, (2) Mokrusha, (3) Vysokogorka, (4) Sadovaya, (5) Gornaya.

Fig. 2. Geological scheme of fragment of Olga ore district (modified and supplemented after F.I. Rostovsky et al., 1981). (*1*) Quaternary deposits; (*2*) Paleocene: Bogopol volcanic complex (rhyolites, rhyodacites, and their tuffs); (*3*, *4*) Late Cretaceous: (*3*) Primorsky volcanic complex (Turonian–Santonian)—tuffs and tuffstones of rhyolites, rhyodacites, (*4*) Sinanchin Formation (Senomanian)—andesites, basaltic andesites, and their tuffs; (*5*) Early Cretaceous (?): sandstone sequence; (*6*) Jurassic system (J_{2-3}): siltstones, tuffites, siliceous rocks, siliceous–clayey shales, sandstones; (*7*) Triassic system: terrigenous–siliceous sequence (T_{2-3}) of Triassic chert formation of Sikhote-Alin consisting of stratified sheeted and lenticular bodies of jaspers, siliceous–rhodochrosite, and manganese silicate rocks, and silicate–magnetite ores; (*8*) Paleozoic (D_3–C_3) limestones, clayey shales, sandstones; (*9*–*13*) Bogopol plutonic complex (Paleocene): dikes of diorites (*9*), andesites (*10*), and basalts (*11*); dikes (*12*) and extrusions (*13*) of rhyolites, rhyodacites, and granite porphyry; (*14*) granitoids of Vladimirsky massif (Maastrichtian–Danian); (*15*–*18*) Primorsky plutonic complex (Turonian–Santonian): (*15*) rhyolite, aplite, and pegmatite dikes, (*16*–*18*) subvolcanic intrusions of diorites (*16*), gabbrodiorites (*17*), and dacites (*18*); (*19*) faults: proved (*a*) and inferred (*b*); (*20*) strike and dip angle of geological boundary; (*21*) iron ore deposit.

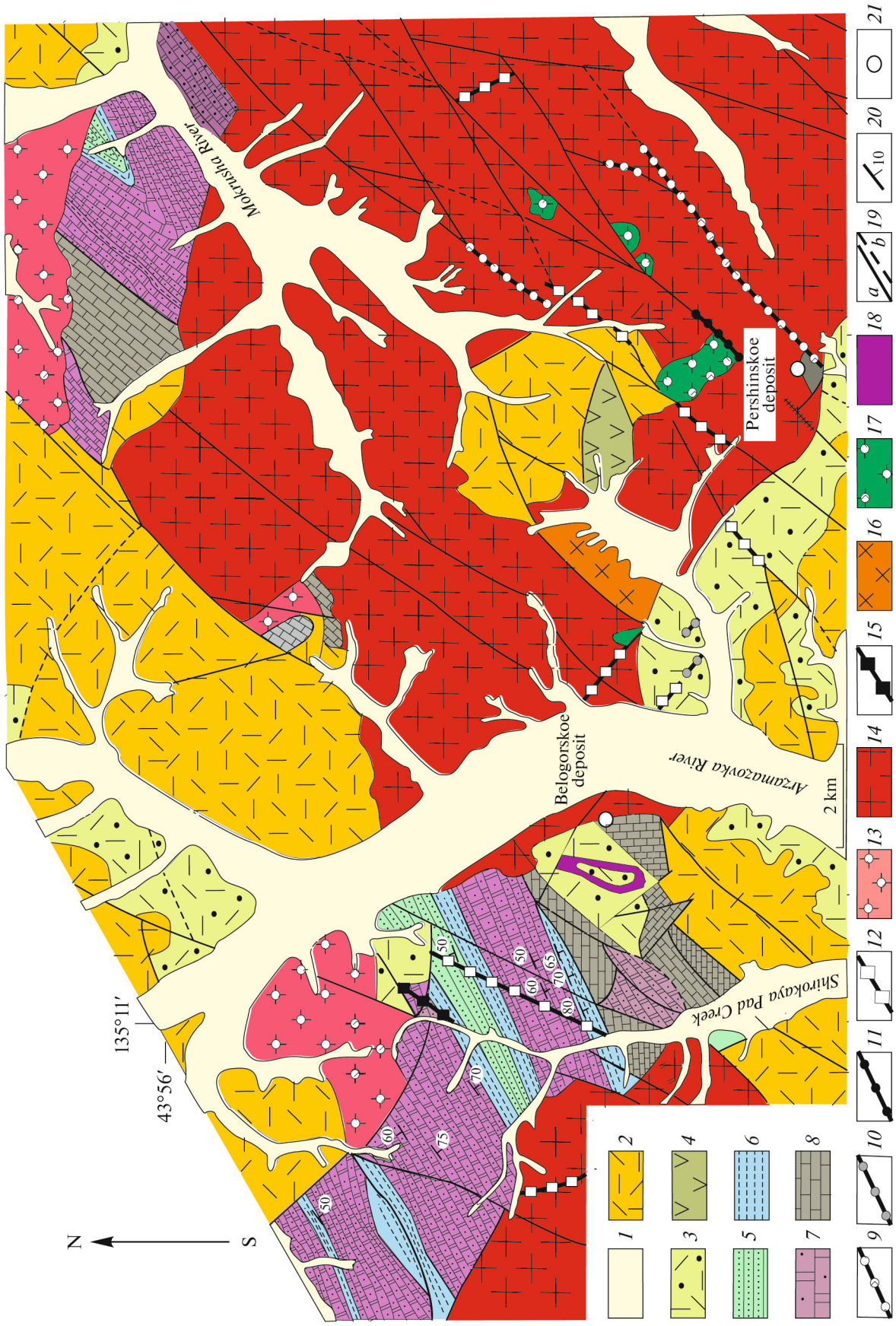
Moktushta River
Pershinskoe deposit
Belogorskoe deposit
Argamazovka River
Shirokaya Pad Creek
2 km
135°11′
43°56′
N
S
1
2
3
4
5
6
7
8
9
10
11
12
13
14
15
16
17
18
19a
19b
20
21

tative analyses were carried out using a PhyRoZ procedure (a standard software of the Link ISIS EDS) with application of user's reference set: $CaMgSi_2O_6$ (blue diopside) for O; Mg, Si, Ca; BaF_2 for F, Ba; Na, $NaAlSi_3O_8$ (albite) for Al; InP for P; FeS_2 for S, Fe; Cs_2ReCl_6 for Cl; $KNbO_3$ for K; Cr_2O_3 for Cr; $MnTiO_3$ for Mn, Ti; Co (metal) for Co; V (metal) for V; ZnS for Zn; $ZrSiO_4$ for Zr; Hf_2O for Hf; $LaPO_4$ for La; $CePO_4$ for Ce; $NdPO_4$ for Nd; $PrPO_4$ for Pr; Pt (metal) for Pt. The Agar Scientific Reference Set was also used. The analytical error (relative standard deviation) did not exceed: (1) ± 10 rel % at element concentrations from 1 to 5 wt %; (2) ± 5 for concentrations from 5 to 10 wt %; (3) ± 2 rel % for concentrations >10 wt %. The detection limit depending on element varied from 0.04 to 0.1 wt %. Samples were sputtered with graphite to provide electric conductivity.

A view on the structural features, relationships of mineral associations, changes of structural features and mineral composition of rocks depending on the degree of manifestation of hydrothermal processes was obtained from detailed study of orebodies in quarry and other mining workings. Obtained results have been reported in detail in published works. In this paper, we focus on the genetic concepts following from them.

RESULTS

Geochemistry

Based on results published in the Pacific Geology in 2022, the average MnO content in the Belogorskaya, Blagodatnaya, and Margaritovskaya orebodies is 4.13 wt % at relatively low REE concentrations (Table 1). The Zn and Cd contents reach 23.08 and 0.12 wt %, at their average contents of 2.17 wt % and 88.04 ppm, respectively. The orebodies have relatively high contents of Sn (up to 651.75 ppm), W (up to 223.2 ppm), Mo (up to 80.44 ppm), Ni (up to 113.22 ppm), and Co (up to 103.57 ppm). The P content in the analyzed samples reaches 1.37 wt %, but in some cases, it is much higher based on apatite content (up to 30–40 vol %). Mineralogical data suggest the relatively high contents of Ag, Te, Sb, and As. Orebodies, as was shown in previous works, have the elevated contents of Au, Pt, and Pd (up to 0.91, 1.54, and 2.35 ppm, respectively).

In the REE patterns, the rocks of the Belogorskoe deposit demonstrate the higher (chondrite-normalized) LREE contents relative to HREE (Fig. 4). Some patterns have sharply expressed positive Eu anomalies and negative Sm anomalies, while others are their variable modifications (see below). The changes were expressed in a decrease of positive Eu anomaly and a negative Sm anomaly up to their complete disappearance and the manifestation of negative Eu anomaly and positive Gd anomaly. In addition, there are distinct bends at Nd or Sm (with flattening patterns toward Nd) or a weakly expressed positive Sm anomaly. Some patterns are flattened and smoothed over the entire length.

Mineralogy

Mineralogy of the deposit was considered by previous researchers [6, 7, 13] and by us [9].

Main Orebodies of the Deposit

Metamorphic Rocks

The oldest rocks of the main orebodies (Blagodatnaya, Belogorskaya, and Margaritovskaya) are represented by massive garnet and banded garnet–magnetite rocks (with usually low amount of apatite, datolite, cuspidine, clinopyroxene, bustamite, or vesuvian).

Rock-Forming Minerals (Major and Subordinate)

Garnet, the concentrator of Sn (up to 2.17 wt % SnO_2), is attributed to the andradite–grossular–spessartine series and sometimes has insignificant contents of Mg, Fe^{+2}, and Ti [9]. The Blagodatnaya and Margaritovskaya orebodies contain abundant andradite with admixture of calderite and koharite end members. Magnetite contains up to 5 mol % jacobsite and 2.00–4.16 wt % ZnO [7, 9]. Clinopyroxene contains up to 16.9–23.9 mol % jahansenite member (at wide variations of Mg and Fe^{+2}) and up to 0.56 wt % Sn. Bustamite is represented by low-Ca and Mn-rich variety close to wollastonite. Datolite contains admixture of Sc, Mg, and Fe—$(Ca_{1.00}Sc_{0.01}Mg_{0.01}Fe_{0.01})_{1.03}B(SiO_4)_{0.97}(OH)$. Apatite in all orebodies is attributed to the Fe-rich variety. The Margaritovskaya orebody contains unusual As-rich (up to 2.65 wt %) variety. Rock-forming minerals of the garnet and magnetite–garnet rocks are characterized in more detail in [9].

Accessory Minerals

Massive garnet and garnet–magnetite rocks contain accessory zircon, baddeleyite, thorianite, thorite, and ilmenite–pyrophanite solid solution. There are also rutile, barite, wolframite, and scheelite. There are also the members of the cobaltite–gersdorffite series, loellingite, and arsenopyrite. Zircon of the Skal'naya orebody contains Sc admixture (Table 2). The extremely rare Th- and U-rich variety was found in the Belogorskaya orebody. The Th- and U-rich zircon with up to 2.15 wt % UO_2 and 1.67 ThO_2 was described in the highly radioactive ultra-potassic melasyenite porphyry of the Czech Republic [44]. Zircons with much higher Th contents (up to 41.8 wt % ThO_2) were found in granites of Germany (Erzgebirge) and Jordan [29], in leucogranites of Albuquergue, USA [23], as well as in the metasomatic rocks of northeastern

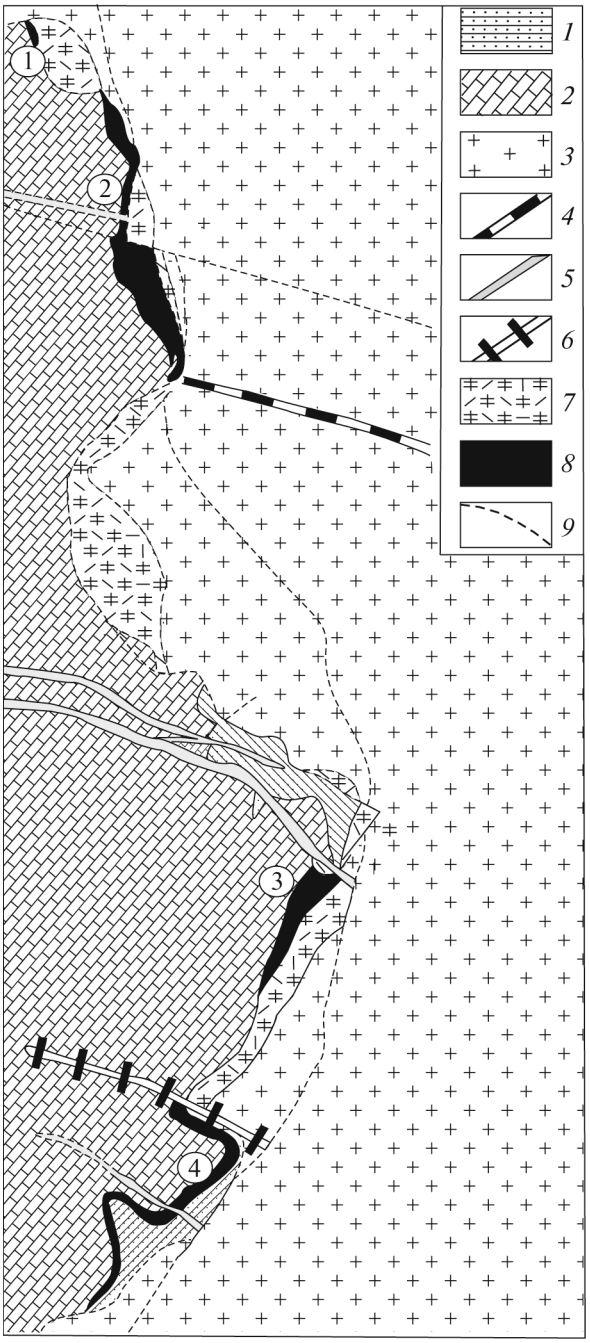

Fig. 3. Geological scheme of Belogorskoe deposit (simplified after I.S. Burdyugova, 1945). (*1*) Early Cretaceous (?) sandstones; (*2*) Middle Carboniferous limestones; (*3*) Late Cretaceous–Paleogene granitoids of Vladimirsky massif; (*4–6*) dikes of basalts (*4*), diorites (*5*), and rhyolites (*6*); (*7*) dacite bodies; (*8*) orebodies: (1–4) (numerals in figure)—Skal'naya (1), Blagodatnaya (2), Belogorskaya (3), and Margaritovskaya (4); (*9*) faults.

Queensland, Australia [24]. Forster considered isomorphous relations in the thorite–xenotime–zircon–coffinite system [29] and proved the existence of complete isomorphous series between zircon and thorite for natural samples. Most of the Th-rich zircons have the high Y and REE contents. Other zircons, including those from the Belogorskaya orebody (Table 2, Fig. 5), are practically or completely devoid of these elements. The presence of Th- and U-rich zircons in the magmatic rocks is thought to be related to the late stages of mineral formation, in particular, to the hydrothermal processes [29, 44]. The Belogorskaya orebody contains the Hf-bearing variety of zircon.

Baddeleyite forms euhedral inclusions in magnetite or garnet without signs of replacement or corrosion (Fig. 6a) and is attributed to the Hf-bearing (up to

Table 1. REE content in Belogorskoe deposit, ppm

Element/ Sample	B-79-2	B-79-16	B-79-26	B-79-28	B-79-31	B-79-32	B-79-33	B-79-37	B-79-38	B-79-48
	1	2	3	4	5	6	7	8	9	10
La	0.6283	0.3408	5.435	3.218	1.418	3.459	1.104	2.400	3.659	1.150
Ce	1.008	0.8480	5.698	5.154	2.426	6.329	3.842	3.388	8.704	2.507
Pr	0.1204	0.09133	0.4727	0.5289	0.4368	1.074	0.3973	0.3887	1.025	0.2489
Nd	0.5618	0.2389	1.452	1.690	2.140	4.633	1.202	1.557	3.006	0.9643
Sm	0.1857	0.09758	0.1187	0.3583	0.3223	0.5180	0.2798	0.3490	0.3187	0.2996
Eu	0.07446	0.03916	0.2354	0.1886	0.0849	0.06150	0.07155	0.0797	0.3061	0.0771
Gd	0.3483	0.1004	0.2887	0.4199	0.3073	0.5045	0.2462	0.5750	0.6198	0.3789
Tb	0.06912	0.03192	0.03153	0.04310	0.0542	0.06726	0.04144	0.2181	0.08145	0.0751
Dy	0.6678	0.1720	0.3185	0.3346	0.3068	0.4329	0.1725	2.328	0.5987	0.6212
Ho	0.1362	0.04198	0.04257	0.06603	0.0687	0.1257	0.06347	0.9004	0.1308	0.1496
Er	0.4638	0.1083	0.1874	0.2401	0.1805	0.4180	0.09395	4.164	0.3579	0.4697
Tm	0.05058	0.02487	0.02665	0.03937	0.0289	0.04907	0.02265	0.8180	0.05288	0.0702
Yb	0.3496	0.1646	0.2128	0.2724	0.1590	0.3367	0.09140	6.103	0.3629	0.3640
Lu	0.04653	0.02765	0.02987	0.04003	0.0226	0.04867	0.02008	0.8710	0.03296	0.0382
Element/ Sample	B-79-55	B-79-59	B-79-62	B-79-84	B-79-85	B-79-88	B-79-92	B-79-94	B-79-96	B-79-98
	11	12	13	14	15	16	17	18	19	20
La	2.353	1.335	1.888	0.4368	1.490	8.463	8.534	5.215	1.723	1.323
Ce	4.818	1.978	9.645	0.6320	2.541	28.733	22.512	10.354	3.318	3.723
Pr	0.7310	0.2298	1.632	0.04884	0.2649	3.785	2.734	1.140	0.4903	0.5730
Nd	2.897	1.016	6.965	0.2012	1.041	12.506	10.572	3.469	1.887	2.066
Sm	0.8939	0.1764	1.937	0.06731	0.3332	1.838	2.326	0.5363	0.5445	0.6313
Eu	0.3284	0.08460	0.1680	0.03712	0.0994	0.1990	0.4858	0.5449	0.1822	0.1436
Gd	1.350	0.3336	1.886	0.09236	0.4288	1.543	2.963	0.6682	0.5990	0.8115
Tb	0.2176	0.07341	0.3195	0.01741	0.09590	0.1987	0.4127	0.1247	0.1117	0.1240
Dy	1.904	0.5238	2.286	0.1065	0.7452	1.282	3.460	0.8920	0.7083	0.8898
Ho	0.4497	0.1356	0.4924	0.02251	0.1958	0.2656	0.6183	0.1916	0.1819	0.2043
Er	1.172	0.3904	1.354	0.1174	0.6191	0.8592	2.009	0.7158	0.5155	0.6701
Tm	0.1798	0.04100	0.2115	0.01797	0.1056	0.1055	0.3160	0.09767	0.06410	0.09570
Yb	0.8609	0.2868	1.410	0.05083	0.6821	0.5084	1.559	0.8032	0.4292	0.6110
Lu	0.1277	0.04172	0.1338	0.01655	0.08408	0.06684	0.1930	0.1009	0.05000	0.05456

Analysts N.V. Zarubina, M.G. Blokhin, and E.V. Elovsky.

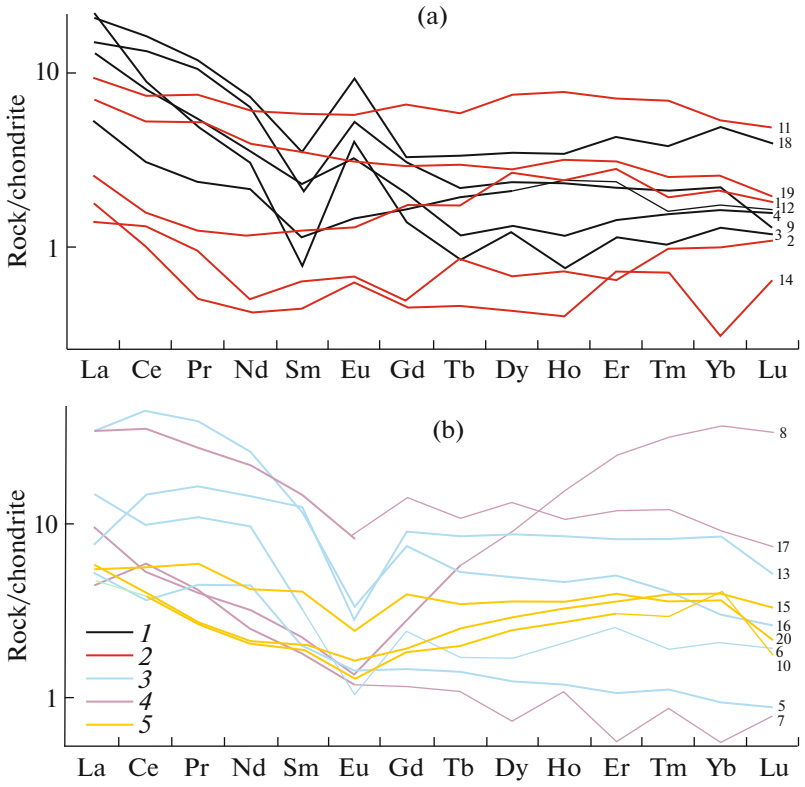

Fig. 4. REE distribution pattern of metamorphic rocks of main orebodies of Belogorskoe deposit. Different color distinguishes spectrum groups based on position of corresponding points relative to trends I and II (see below Fig. 10b): (1, 2) plotted in trend II (or near it) within (1) or beyond (2) possible Sm/Nd ratios for gabbroids of Vladimiro–Aleksandrovsky massif (a); (3–5) located at trend 1 (4), below (3), or above (5) it (b). Pattern numbers correspond to ordinal numbers in Table 1.

1.20 wt %) variety (Table 2). This relatively rare mineral is known in carbonatites, kimberlites, impact melt rocks, impact structures, alkaline syenites, apatite–forsterite, and dolomite–phlogopite rocks, magnetite ores, layered mafic intrusions, diabase dikes, gabbro sills, anorthosites, and some other rocks. It has much higher melting temperature compared to zircon [1]. In this relation, the appearance of baddeleyite instead of zircon can be caused by the extremely high temperature or low Si content in the system. In addition, its formation could be caused by the presence of strong bases (Mg or Ca) that are able to bind all Si with formation of quartz-free associations. At the Belogorskoe deposit, baddeleyite was found in quartz-free magnetite- and garnet-rich interlayers of the banded garnet–magnetite rocks.

Thorianite forms accumulations of small crystals in garnet, without signs of replacement or corrosion. It contains insignificant amounts of Zr and U (Table 2). Based on microprobe data, rutile forms small euhedral grains in garnet and contains V, Zr, and Sc– $(Ti_{0.98}V_{0.008}Sc_{0.005}Zr_{0.007})_{1.00}O_2$.

The ilmenite–pyrophanite solid solution is characterized by the approximately equal amount of ilmenite and pyrophanite end members [9]. It occurs as typical accessory mineral in the products of prograde metamorphism of manganese sediments, as in the garnet and garnet–magnetite rocks of the Belogorskoe deposit [15, 33]. At the retrograde stage, pyrophanite was exsolved from solid solutions as inclusions in hematite [20, 26], magnetite [37], and jacobsite [40]. In diverse magmatic and metamorphic rocks, as at the Belogorskoe deposit, magnetite usually associates with Fe-rich members of the ilmenite—pyrophanite series (ilmenite, manganoilmenite, more rarely, Fe-rich pyrophanite), whereas in association with hematite, this mineral contains no Fe^{+2}, but is slightly enriched in Fe^{+3}. Barite is peculiar in the presence of Sr. Wolframite $(Mn_{0.22–0.93}Fe_{0.81–0.07})_{1.03–1.00}(WO_4)_{0.97–1.00}$ and scheelite $(Ca_{0.85–1.02}Sr_{0.24–0.00})_{1.09–1.02}(WO_4)_{0.91–0.98}$ form euhedral inclusions in early minerals without signs of replacement or corrosion. Formulas of these minerals are given based on results of microprobe analysis.

The composition of mineral of the cobaltite–gersdorffite isomorphous series (with significant admixture of ferroan member) changes from composition of Co-rich gersdorffite to Ni-depleted cobaltite (Table 2). It associates with Ni-bearing loellingite, Ni_2As_3, and nickeline. There are data on the existence of complete solid solution between loellingite and isostruc-

Table 2. Composition of accessory minerals of Belogorskoe deposit (wt %)

No.	O	Si	Al	Fe	Mn	Ca	S	Co	Ni	As	Ba	Zr	Th	U	La	Ce	Total	Formulas
1	25.40											70.60					97.25	$(Zr_{0.99}Hf_{0.01})_{1.00}O_2$
2	34.62	13.34	0.87	4.73								28.1	11.34	3.54			97.09	$(Zr_{0.83}Th_{0.13}U_{0.04})_{1.00}SiO_4$
3	34.38	12.69		0.87								31.4	14.71	3.49			97.54	$(Zr_{0.79}Th_{0.16}U_{0.03})_{0.98}(SiO_4)_{1.02}$
4	34.68	15.06										46.32					97.44	$(Zr_{0.96}Hf_{0.02})_{0.98}(SiO_4)_{1.02}$
5	34.26	14.98		0.34		0.53						47.73					98.37	$(Zr_{0.98}Sc_{0.02})_{1.00}(SiO_4)_{1.00}$
6	13.75											2.14	83.49	1.86			101.24	$(Th_{0.91}Zr_{0.07}U_{0.02})_{1.00}O_2$
7	32.17	1.65	0.86			3.72							6.05	1.42	12.46	22.31	100.97	$(Ce_{0.39}Ca_{0.22}La_{0.22}Nd_{0.13}$
																		$(Th_{0.06}U_{0.01})_{1.03}(PO_4)_{0.97}$
8	37.60	14.84	9.15	7.89	3.1	7.12									4.7	9.7	96.96	$(Ca_{1.04}Mn_{0.19}La_{0.20}Ce_{0.40}Nd_{0.12})_{1.95}$
																		$(Al_{1.99}Fe_{0.83}Mn_{0.14})_{2.96}Si_{3.09}O_{12}(O,OH)$
9	28.2	21.01									49.57						99.49	$(Ba_{0.97}Cu_{0.03})_{1.00}Si_{2.00}O_{4.72}$
10	27.54	20.72						0.17			49.74						98.17	$(Ba_{0.99}Co_{0.01})_{1.00}Si_{2.00}O_{4.68}$
11	3.47	0.37		4.97		1.25	20.28	26.38	3.97	41.99							102.86	$(Co_{0.75}Ni_{0.11}Fe_{0.14})_{1.00}As_{0.94}S_{1.06}$
12	5.54	2.73		6.83	1.8		15.97	7.78	19.08	42.04							101.15	$(Co_{0.25}Ni_{0.61}Fe_{0.14})_{0.90}As_{1.06}S_{0.94}$
13	7.08	3.53		25.89		2.86	0.53		0.48	60.97							101.34	$(Fe_{0.98}Ni_{0.02})_{1.00}(As_{1.96}S_{0.04})_{2.00}$
14				1.94			1.46	1.63	31.11	64.03							100.17	$(Ni_{1.79}Fe_{0.12}Co_{0.09})_{1.99}(As_{2.86}S_{0.15})_{3.01}$
15				0.41		0.68		0.66	44.54	52.28							98.57	$(Ni_{0.97}Co_{0.01}Fe_{0.01})_{0.99}As_{1.01}$
16				0.34		0.61			45.01	54.2							100.16	$Ni_{1.03}As_{0.97}$

Orebodies: Belogorskaya (1–4, 6), Blagodatnaya (11, 13), Skal'naya (5, 7–10, 12, 14–16). Minerals: baddeleyite (1), zircon (2–5), thorianite (6), monazite (7), allanite (8), sanbornite (9, 10), cobaltite–gersdorffite (11, 12), loellingite (13), Ni_2As_3 (14), nickeline (15, 16). An. 1 and 4, in addition, include 1.25 and 1.38 wt % Hf, respectively; an. 2—0.55 Mg; an. 5—0.53 Sc; an. 7—8.02 Nd and 12.31 P; an. 8—2.86 Nd; an. 9—0.71 Cu.

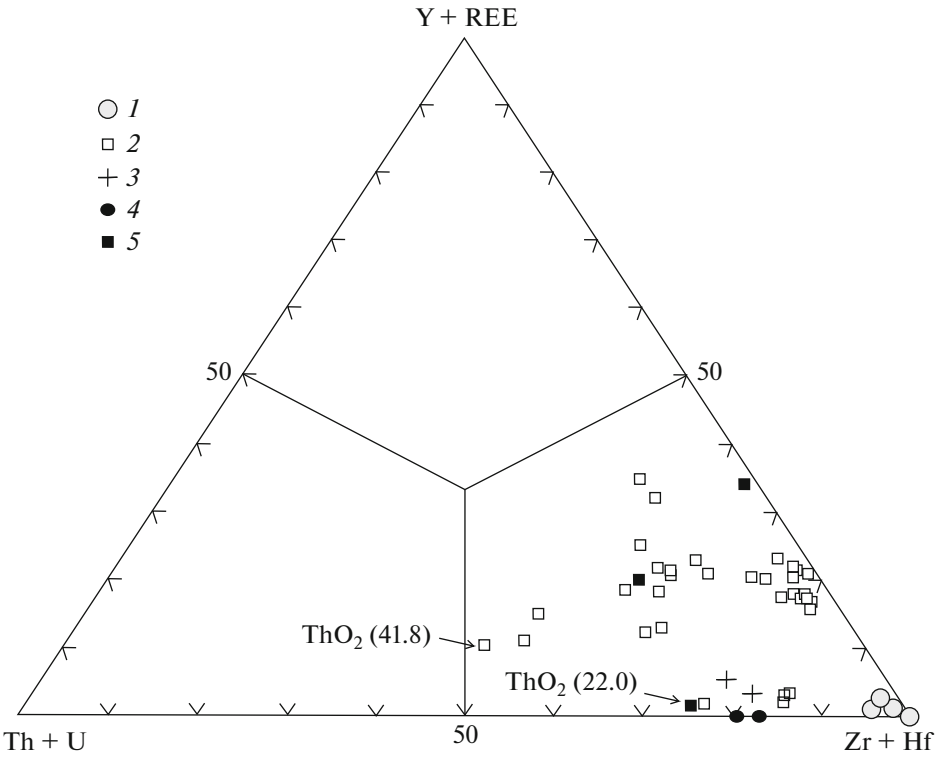

Fig. 5. Diagram (Zr,Hf)–(Y,REE)–(U,Th) [29] for zircon with some additions. (*1*) From highly radioactive ultrapotassic melasyenite porphyry of Czechia [44]; (2, 3) from granites of Germany (Erzgebirge) (*2*) and Jordan (*3*) [29]; (*4*) from Belogorskoe deposit; (*5*) from leucogranites of Albuquerque, USA [23] and metasomatic rocks from northeastern Queensland, Australia [24].

tural rammelsbergite in some low-temperature rocks [5].

The rock-forming minerals of garnet and garnet–magnetite rocks form intergrowths, while accessory minerals occur as inclusions in them, without signs of corrosion or replacement (Figs. 6a–6c).

Products of Hydrothermal Alteration of Metamorphic Rocks

Rock-Forming Minerals (Major and Subordinate)

Garnet and garnet–magnetite rocks contain later minerals. The most abundant of them are massive magnetite, calcite, with less common fluorite and sphalerite. They compose segregations of different morphology and mineral composition: (1) small calcite pockets dispersed in garnet and garnet–magnetite rocks; (2) blocks of massive magnetite; (3) pockets of coarse-crystalline calcite with subordinate amount of fluorite and short veins of sphalerite in the magnetite blocks and near them; (4) amphibole–rhodonite segregations (sometimes with calcite or fluorite) near carbonate pockets; (5) systems of calcitic (with relicts of garnet and, sometimes, with amphibole, rhodonite, or fluorite) veinlets cutting across altered garnet and garnet magnetite rocks.

Massive magnetite is characterized by the high content of the jacobsite member (up to 33 mol %) [9]. Sphalerite in the pockets of coarse-crystalline calcite is represented by brown or green Fe-depleted or Fe-free varieties. Calcite contains small amount of rhodochrosite, siderite, and magnesite members. Amphibole is attributed to the tremolite–ferroactinolite series and is enriched in Mn. Rhodonite in association with amphibole (± calcite, fluorite) is represented, as was shown in previous works, by Fe-depleted moderate-Ca variety.

Accessory Minerals

The alteration products of garnet and garnet–magnetite rocks also contain diverse accessory minerals. They are present in the magnetite blocks and pockets of coarse-crystalline calcite, as well as occur in altered rocks and systems of calcite veinlets and thin veins intersecting them.

Massive magnetite that composes magnetite blocks usually contains microinclusions of cassiterite, which was formed owing to Sn presence in garnet, while calcite and fluorite in calcite pockets from magnetite blocks contain microinclusions of bismuth minerals, molybdenite, and members of the scheelite–powellite isomorphous series (Figs. 7a–7c). The bismuth minerals, in addition, occur as small pockets and dissemi-

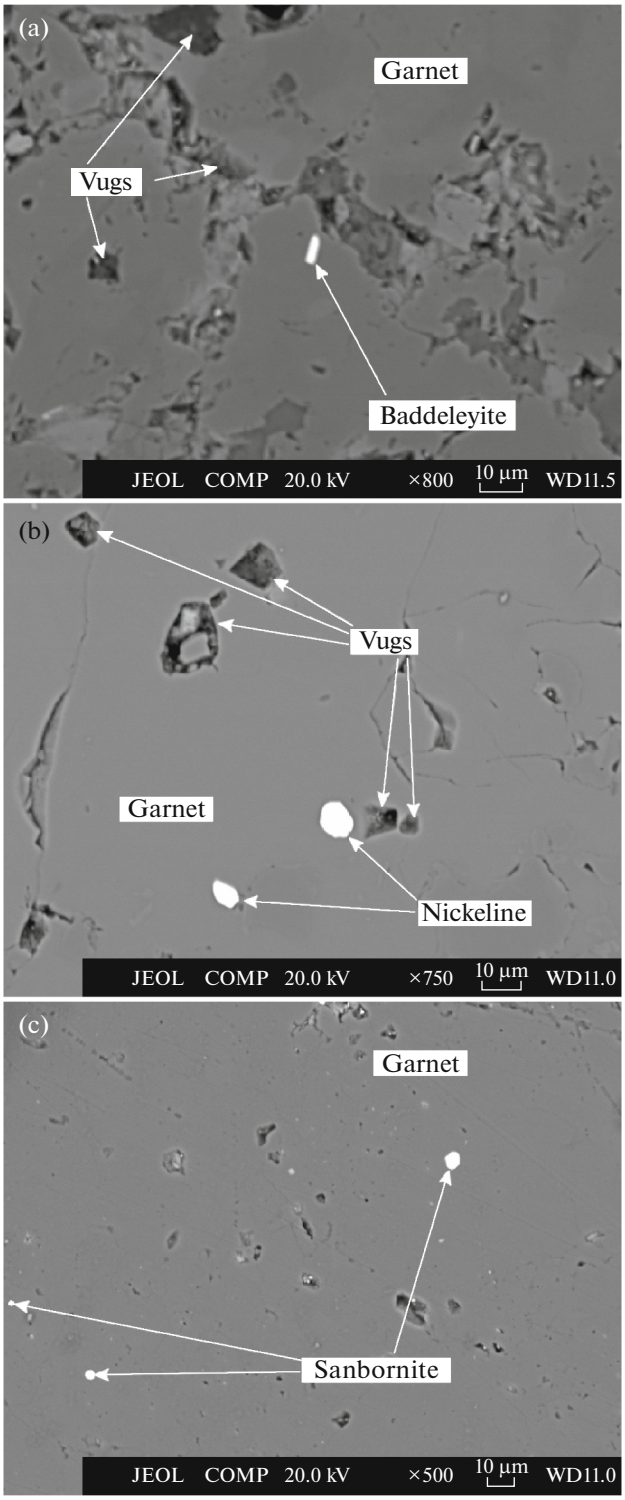

Fig. 6. Inclusions of baddeleyite (a), nickeline (b), and sanbornite (c) in garnet. Belogorskaya (a) and Skal'naya (b, c) orebodies.

nation in rhodonite. In the altered rocks and intersecting systems of thin calcite veinlets, we found galena, sphalerite, pyrite, chalcopyrite, arsenopyrite, gudmundite, ullmannite, stannite, sulfosalts, stibnite, native Sb, and other minerals.

The bismuth minerals occur in calcite, fluorite, and rhodonite, or at the contact of calcite and fluorite pockets with earlier garnet (Figs. 7a, 7b). In the calcite and fluorite, they form individual crystals (tens to hundreds μm in size) and intergrowths with each

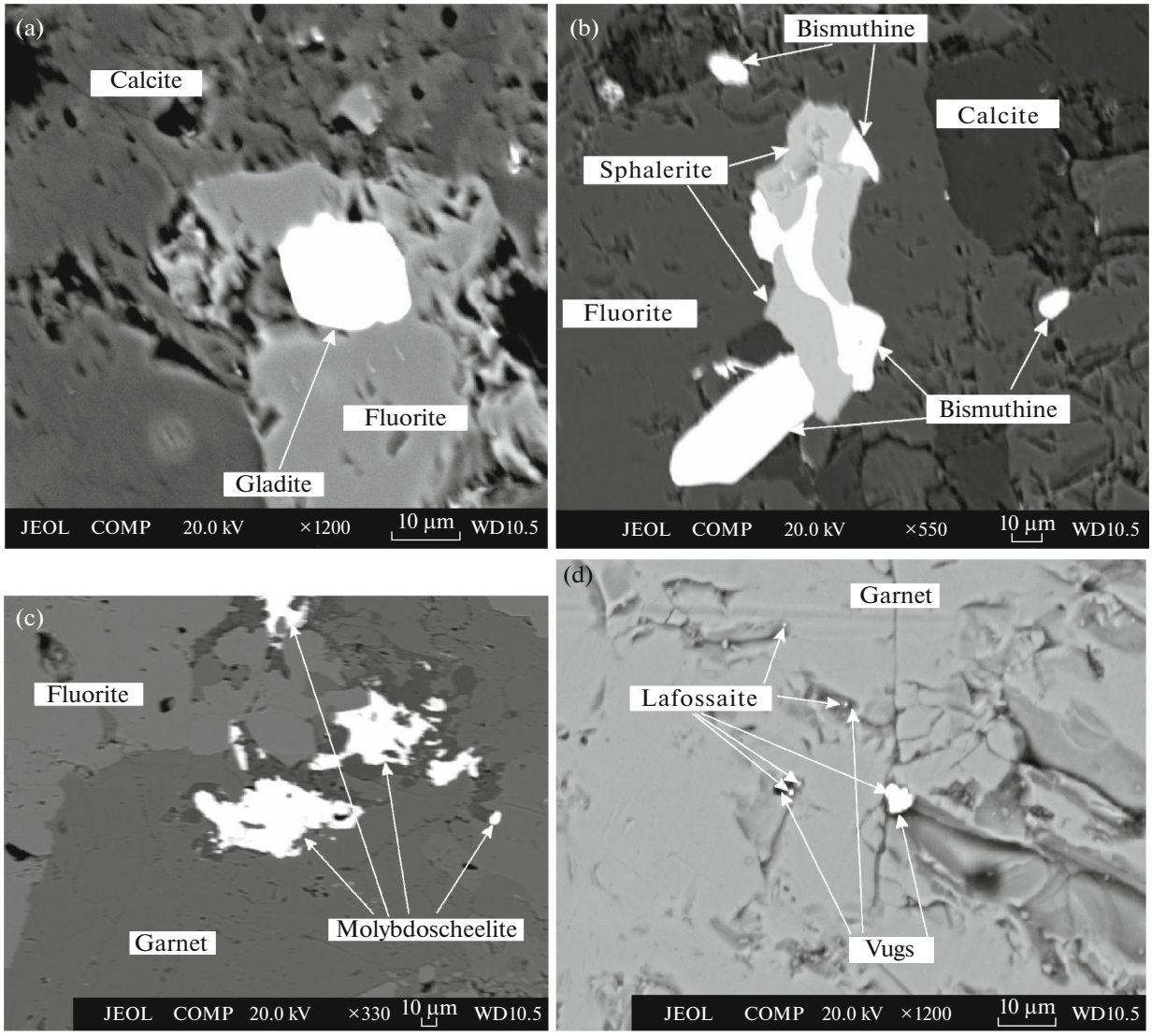

Fig. 7. Crystals of gladite (bright) (a), intergrowths of Bismuthine (bright) and sphalerite (gray) in fluorite (b), calcite–molybdoscheelite aggregates in fluorite and garnet (c), and grains of lafossaite (d) in cavities of exogenic leaching of garnet rock. Blagodatnaya (a, b) and Margaritovskaya (c, d) orebodies.

other, sphalerite, galena, or compose elongate areas along cleavage planes. The bismuth mineralization is represented by native Bi, bismutite, joseite A, cosalite, gladite, jonassonite $AuBi_5S_4$ (first find in Sikhote-Alin), and galenobismutite. There are also compounds Bi_3Te_2, (Bi,Ag)(S,Te), Bi_3S_4, (Pb,Ag)BiS_2, Bi_2Te, Bi_4Te, Bi_5Te, and Bi_6Te, which were described in the geological literature but have no own names.

Similarly, bismuth mineralization and jonassonite of the Belogorskoe deposit were described in detail in our publications in 2022.

The pockets of coarse-crystalline calcite, in addition to bismuth minerals, contain molybdenite and members of the scheelite–powellite series $Ca_{1.03-0.98}(W_{0.79-0.01}Mo_{0.21-1.01})_{0.97-1.02}O_4$. They form intricate intergrowths of irregular shape with each other and with sphalerite in the alteration products of early associations together with carbonate or fluorite (Fig. 7c), but more frequently occur as individual pockets and stringer in these minerals.

The altered garnet and garnet–magnetite rocks and cross-cutting calcite veinlets contain Fe- and Mn-free sphalerite (Table 3), Ag-rich tetrahedrite, polybasite, cinnabar, coloradoite, $Ag_4Sb_2S_3$(?) (or based on analysis of $Ag_{4.01}Sb_{2.00}S_{2.98}$), ullmannite, stibnite, as well as native Sb. The polybasite is enriched in pearceite member, while ullmannite contains insignificant amounts of Co. Pyrite, bournonite, robinsonite, heteromorphite, and $Pb_2Sb_2S_5$ (Table 3) occasionally occur. The last mineral likely represents As-free analogue of veenite with an ideal formula $Pb_2(Sb,As)_2S_5$ [25, 31, 36]. The $Pb_2Sb_2S_5$ compound is sometimes

Table 3. Compositions of sulfides, sulfosalts, and other minerals in hydrothermal and exogenic (*) alteration products of garnet and garnet–magnetite rocks of Belogorskoe deposit (wt %)

No.	Si	S	Cl	Ca	Fe	Cu	Zn	Tl	Ag	As	Sb	Pb	Total	Mineral	Formulas
1		21.10			6.95	15.57	0.62		28.05		24.57		97.31	Fahlore	$(Cu_{9.28}Ag_{10.01}Zn_{0.36}Fe_{4.71})_{24.36}Sb_{7.64}S_{24.92}$
2		50.37		0.06	43.48					3.55			97.46	Pyrite	$Fe_{0.97}(S_{1.97}As_{0.06})_{2.03}$
3		19.44			0.22	12.95					24.70	41.84	99.15	Bournonite	$Pb_{1.00}Cu_{1.01}Sb_{1.00}S_{2.99}$
4		20.69		0.05	0.09						36.22	41.08	98.13	Robinsonite	$Pb_{3.99}Sb_{6.00}S_{13.01}$
5		29.07									70.90		99.97	Stibnite	$Sb_{1.96}S_{3.04}$
6	0.19	15.14			29.08					2.06	52.40		98.87	Gudmundite	$Fe_{1.07}(Sb_{0.89}As_{0.06})_{0.95}S_{0.98}$
7		33.09		0.4			66.24						99.73	Sphalerite	$Zn_{1.01}S_{0.99}$
8			13.30		0.44			85.21					98.95	Lafossaite	$Tl_{1.05}Cl_{0.95}$

Orebodies: Belogorskaya (1), Blagodatnaya (2–6), Margaritovskaya (7), and Skal'naya (8).

mentioned in literature as "plumosite" or considered as Fe-free variety of jamesonite. Pyrite is attributed to the As variety. Gudmundite, a relatively rare mineral, contains isomorphous admixture of As (Table 3).

Skal'naya Orebody

In the Skal'naya orebody, early associations are made up of garnet, pyroxene, and bustamite. As accessory minerals, they contain ilmenite–pyrophanite solid solution, titanite, zircon, monazite, allanite, sanbornite, perovskite, rutile, apatite, barite, and phosphate $InPO_4$. There are also diverse Ni compounds: Ni_2As_3, nickeline, loellingite, ullmannite, and cobaltite–gersdorffite (Table 2). Garnet is attributed to the grossular–spessartine variety sometimes enriched (up to 24.3 mol %) in andradite member [9]. Pyroxene is attributed to the diopside–hedenbergite–johannsenite series with variable content of johannsenite member (16.9–23.9 mol %). With rare exception, it is enriched in diopside (31.2–37.4 mol %) and relatively depleted in hedenbergite (43.3–49.1, rarely up to 65.6 mol %). Sometimes, the pyroxene contains Zn (up to 0.40 wt %). The bustamite occurs together with clinopyroxene. It is attributed to the Mg-rich and the lowest-Ca variety. The ilmenite–pyrophanite solid solution is present as dispersed tabular crystals. Its composition widely varies from almost "pure" pyrophanite (88.9 mol % $MnTiO_3$) to Mn-rich ilmenite (69.4 mol % $FeTiO_3$). The ilmenite–pyrophanite solid solution is frequently enriched in V and Nb. Zircon is represented by an Sc-bearing variety (Table 2). Monazite is enriched in LREE. It contains an isomorphous admixture of Th and U and belongs to the cheralite–monazite isomorphous series, which is characterized by the heterovalent isomorphism according to a scheme $CaTh \rightarrow 2REE$. Allanite is represented by an Mn- and REE-rich variety. Sanbornite (Fig. 6c), a rare barium silicate [42], at the Belogorskoe deposit contains an admixture of Cu, more rarely Cu and Co, or only Co (Table 2). Microprobe analysis showed that perovskite contains an insignificant admixture of Fe and Al: $Ca_{1.02}(Ti_{0.95}Fe_{0.01}Al_{0.02})_{0.98}O_3$. Titanite contains insignificant amounts of Al at the Ti site: $Ca_{1.03}(Ti_{0.86}Al_{0.11})_{0.97}Si_{1.00}O_4(O,OH)$. Rutile corresponds to the V-, Sc-, and Zr-bearing variety $(Ti_{0.98}V_{0.008}Sc_{0.005}Zr_{0.007})O_2$. Apatite from the Skal'naya orebody contains an Sc admixture. Phosphate $InPO_4$ is likely attributed to previously unknown natural compounds. It was found as artificial chemical matter. Arsenide Ni_2As_3 is enriched in Co, which substituted Ni, and in particular, in S occupying the As site (Table 2). This mineral has the variable composition $(Ni_{1.81–1.91}Co_{0.10–0.12})_{1.91–2.03}(As_{2.93–2.24}S_{0.16–0.73})_{3.09–2.97}$. Ullmannite contains an insignificant admixture of Co.

The alteration products of early assemblages of the Skal'naya orebody mainly consist of carbonate, amphibole, manganous chlorite, and manganaxinite. These minerals contain inclusions of native Bi and $(Pb,Ag)BiS_2$. Based on previous research, carbonate is represented by manganoan calcite (up to 12 mol % rhodochrosite) [9]. Amphibole of the tremolite–ferroactinolite series that developed after clinopyroxene is also enriched in Mn (up to 2.90 wt %). Mn- and Fe-rich amphibole of the cummingtonite–grunerite series occasionally occur. Axinite is enriched in Mn: $(Ca_{1.79}Mn_{0.21})_{2.00}(Mn_{0.74}Fe_{0.20})_{0.94}Al_{2.05}BSi_{4.01}O_{15}(OH)$ and attributed to the manganaxinite–tinzenite isomorphous series.

The Belogorskoe deposit is peculiar in the presence of the Au–Ag–Pd–Pt mineralization. Noble metal minerals were found both in early assemblages and their alteration products in all orebodies. They are represented by native Au without admixtures, Au–Ag solid solution, platinum Au, and disordered Au-based Cu–Ag–Au solid solutions. There are also disordered solid solutions or likely intermetallides Cu_2Au,$Cu_4(Au,Ag)_3$, $CuAu_2$, Pd_3Ag, as well as Pd_4Ag, PdPt, native Pt, Ag sulfide, Ag-rich tetrahedrite, polybasite, the aforementioned Ag compounds with Bi, Te, and Sb, as well as other minerals. The Au–Ag–Pd–Pt mineralization is considered in detail in our publication in *VGU Vestnik* in 2019.

Oxidation Zone

The Blagodatnaya, Belogorskaya, and Margaritovskaya orebodies contain preisingerite, bastnaesite, bismite, dobreite, zavartskite, ilzemanite, lafossaite, massicot, and other exogenic minerals. The exogenic origin of lafossaite (Table 3) is confirmed by its confinement to the exogenic leaching cavities of endogenic crystals (Fig. 7d). Lafossaite, characterized as a new mineral from the La Fossa crater (Italy) [39], has been recently found in exhalations of the Avacha volcano [14].

DISCUSSION

According to earlier data, the metamorphosed Triassic metalliferous sediments and calc-silicate rocks (regarded as skarn) of the deposits of the Taukha terrane are the contact-metamorphosed and partially regenerated erosion products in the Triassic apogabbroid laterite weathering crust on islands. Mn, Fe, and other metals accumulated in lagoons and basins around the islands. The presence of boron and base-metal ores in calc-silicate rocks indicates shallow (drying) and deep-water (with zones of H_2S contamination) lagoons. The lagoonal facies (presently, calc-silicate rocks) and basin facies (metamorphosed metalliferous sediments of the Triassic chert formation), despite significant sedimentary differentiation, revealed, as shown in earlier studies, the geochemical features of the magmatic source rocks.

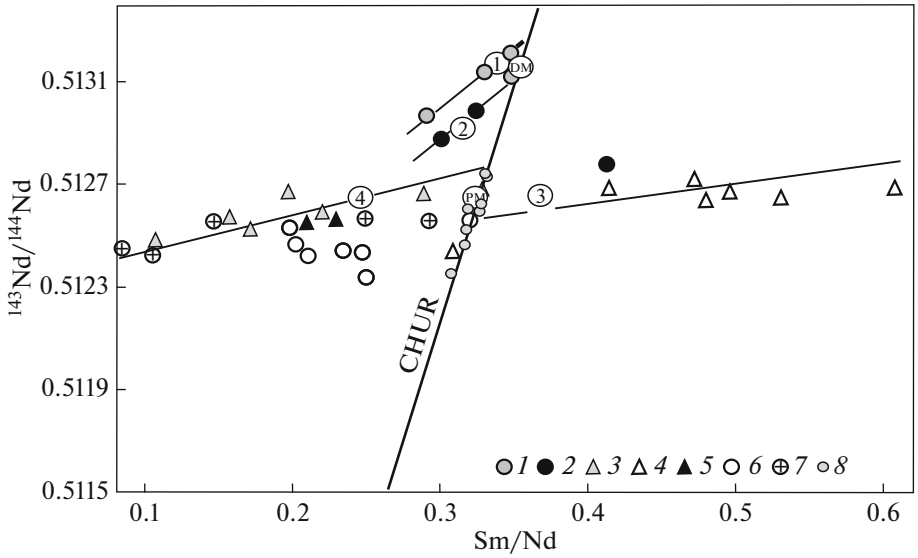

Fig. 8. Position of data points of metamorphic rocks of Belogorskoe deposit in diagram $^{143}Nd/^{144}Nd$–Sm/Nd [10]. (1, 2) Mafic rocks of Avdokimovsky complex from inclusions in rocks of Sergeevsky complex (1), peridotites of massif near Dalny Kut village (unknown age) (2); (3–6) dunites, troctolites, and anorthosites of Vladimiro–Aleksandrovsky massif (Cambrian) (3), troctolites, olivinites, and other rocks of Breevka allochthon (Kalinovsky complex, Paleozoic) (4), Kamenka (5) and Sergeevsky (6) gabbro (Sergeevsky complex, Cambrian); (7) rocks of Belogorskoe deposit; (8) chondrites; DM and PM (in circles) are depleted and primitive mantle, respectively; circled numerals are numbers of trends. Starting data for rocks of Belogorskoe deposit are listed in Tables 1 and 4.

The alignment of data points to delineate certain trends (1–4) in the $^{143}Nd/^{144}Nd$–Sm/Nd diagram (Fig. 8) does not depend on the petrochemical features of magmatic rocks, but is determined only by their age and type of mantle source [10]. Data points of the main orebodies of the Belogorskoe deposit in this diagram plot along trend 4. Their position unambiguously indicates that their source was the Sergeevsky Complex or gabbroids similar in isotope and geochemical composition to the rocks of the Vladimiro–Aleksandrovsky massif, as well as the absence of significant Sm and Nd fractionation in the protoliths (sediments) compared to the source rocks. The position of almost all data points of the Sergeevsky gabbro beyond trend 4 is related to a change in the $^{143}Nd/^{144}Nd$ and Sm/Nd ratios after the formation of Triassic sediments (during Middle–Late Jurassic accretion) owing to seawater-related metamorphism [10].

The specific features of the chondrite-normalized REE patterns of samples (3, 4, 9, 12, 18, Fig. 4a), such as LREE enrichment with respect to HREE, as well as positive Eu anomalies and negative Sm anomalies, unambiguously point to the gabbroids geochemically similar to the studied rocks of the Vladimiro–Aleksandrovsky massif (Fig. 9e). This conclusion is also confirmed by their arrangement along trend II in the diagram Sm/Nd–Sm/Eu (Fig. 10b).

Based on the REE distribution patterns (Figs. 4a, 4b) and position of data points in the diagram (Fig. 10b), other samples correspond to the products of exogenic decomposition of gabbroids, initial (gabbroid) values of Sm/Nd and Sm/Eu in which were modified by the interaction with seawater (during sedimentation, diagenesis, or Late Jurassic–Early Cretaceous accretion), hydrothermal processes, or interaction with seawater and hydrothermal processes. Samples 2, 14 of them are metamorphosed sediments that likely experienced only intense hydrothermal alter-

Table 4. Geochemical and isotope Sm-Nd characteristics of rocks of Belogorskoe deposit

No.	Sample	Sm	Nd	Sm/Nd	$^{143}Nd/^{144}Nd$	Err
1	Б-79-26	0.0775	1.4039	0.055	0.512478	19
2	Б-79-32	0.4646	4.4208	0.105	0.512422	16
3	Б-79-55	0.7784	2.6682	0.292	0.512560	11
4	Б-79-88	1.7285	12.1191	0.143	0.512560	11
5	Б-79-92	1.8423	7.3608	0.250	0.512572	18

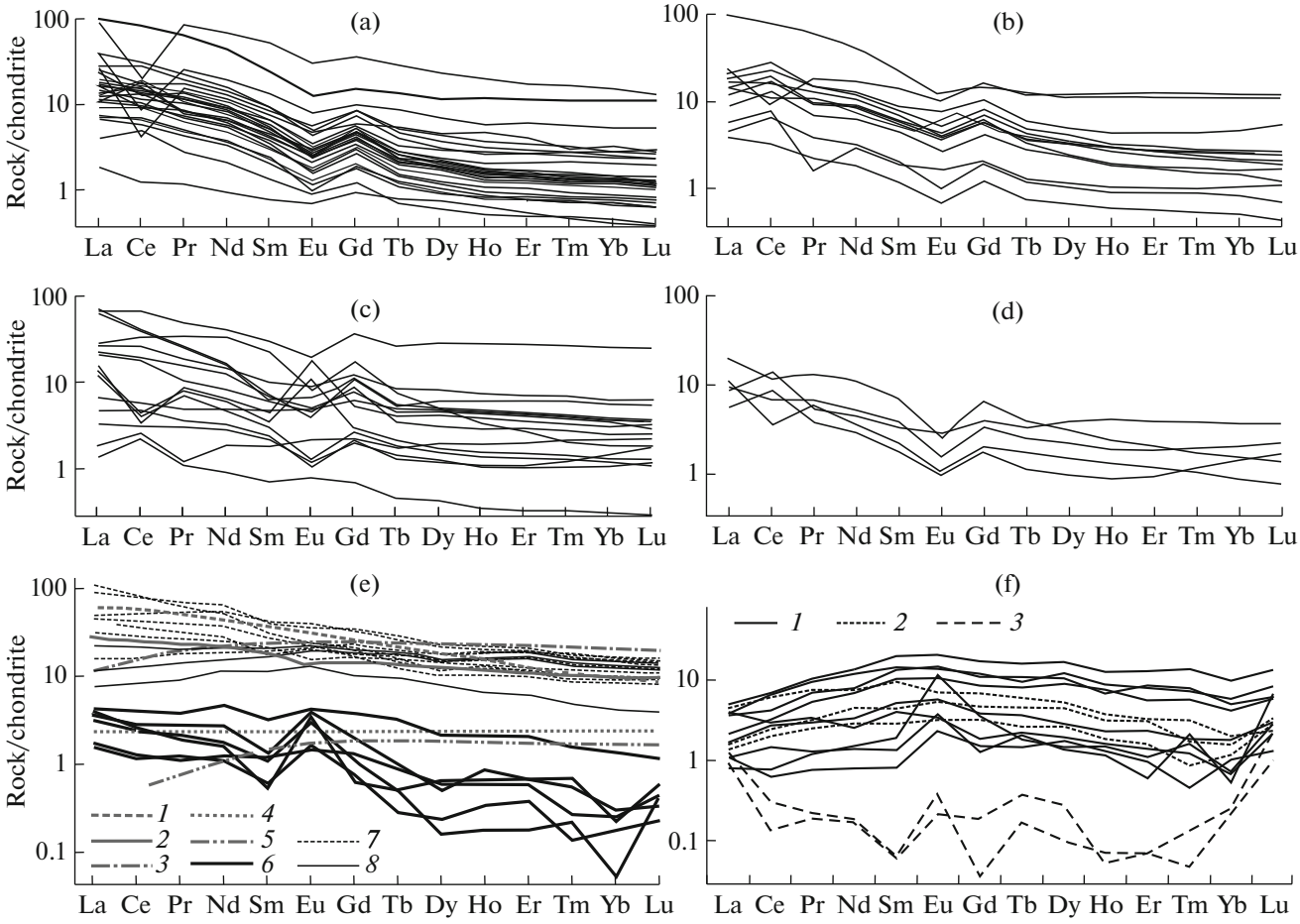

Fig. 9. REE distribution patterns of studied rocks and ores of Sikhote-Alin. Rocks and ores of Triassic chert formation of Sikhote-Alin (a–d): jaspers (a), manganese silicate rocks (c), and silicate–magnetite ores (d) of Shirokaya Pad area, manganese silicate rocks of Gornaya area (b). Magmatic rocks of basic–hyperbasic complexes of Sikhote-Alin (e, f): e (1–8) OIB (1), IAB (2), MORB (3), primitive (4) and depleted (5) mantles, gabbroids of Vladimiro–Aleksandrovsky massif (6), Sergeevsky (7) and Avdokimovsky complexes (8); f (*1–3*) gabbroids of Kalinovsky Complex (Breevka allochthon) (*1*) and Dalny Kut massif (*2*); (*3*) serpentinites of Melkovodnaya Bight. Reference patterns were plotted using geochemical data [41] (for OIB and MORB); [34] (for IAB); [35, 43] (for primitive mantle); [38] (for depleted mantle). REE contents in studied rocks were normalized to chondrites according to [27].

ations. Their data points plot on the continuation of the trend of the Vladimiro–Aleksandrovsky gabbroids, above possible Sm/Nd ratios in these rocks (0.325), while REE patterns retained positive Eu anomaly (Fig. 4a). Other samples are metamorphosed sediments, the initial (gabbroid) Sm/Nd and Sm/Eu values in which were variably modified, supposedly under the influence of seawater and hydrothermal solutions. Due to the influence of seawater, their patterns (Fig. 4b) show typical features of jaspers and metamorphosed analogues of metalliferous sediments of the Triassic chert formation of Sikhote-Alin: manganese silicate rocks and silicate–magnetite ores (Figs. 9a–9d). These features are the higher (chondrite-normalized) LREE contents relative to the HREE and the presence of negative Eu and positive Gd anomalies.

As earlier studies have shown, the metals were supplied into protoliths (sediments) of jaspers, manganese silicate rocks, and silicate–magnetite ores as colloidal Mn and Fe hydroxides, and, accordingly, the REE distribution patterns in these rocks correspond to those of seawater during sedimentation. This explains the predominant arrangement of data points of these rocks in the Sm/Nd–Sm/Eu diagram (Fig. 10b) to trend I with an Sm/Nd ratio close to the present-day value in seawater of 0.21 [21, 28]. The data points of the Sergeevsky mafic rocks that were metamorphosed with seawater assistance during Middle Jurassic accretion and some data points (7, 8, 17) of the studied rocks of the Belogorskoe deposit are also arranged along this trend (Fig. 10). The influence of seawater on the Sm/Nd and Sm/Eu ratios is likely explained by a significant shift of data points of some samples of the

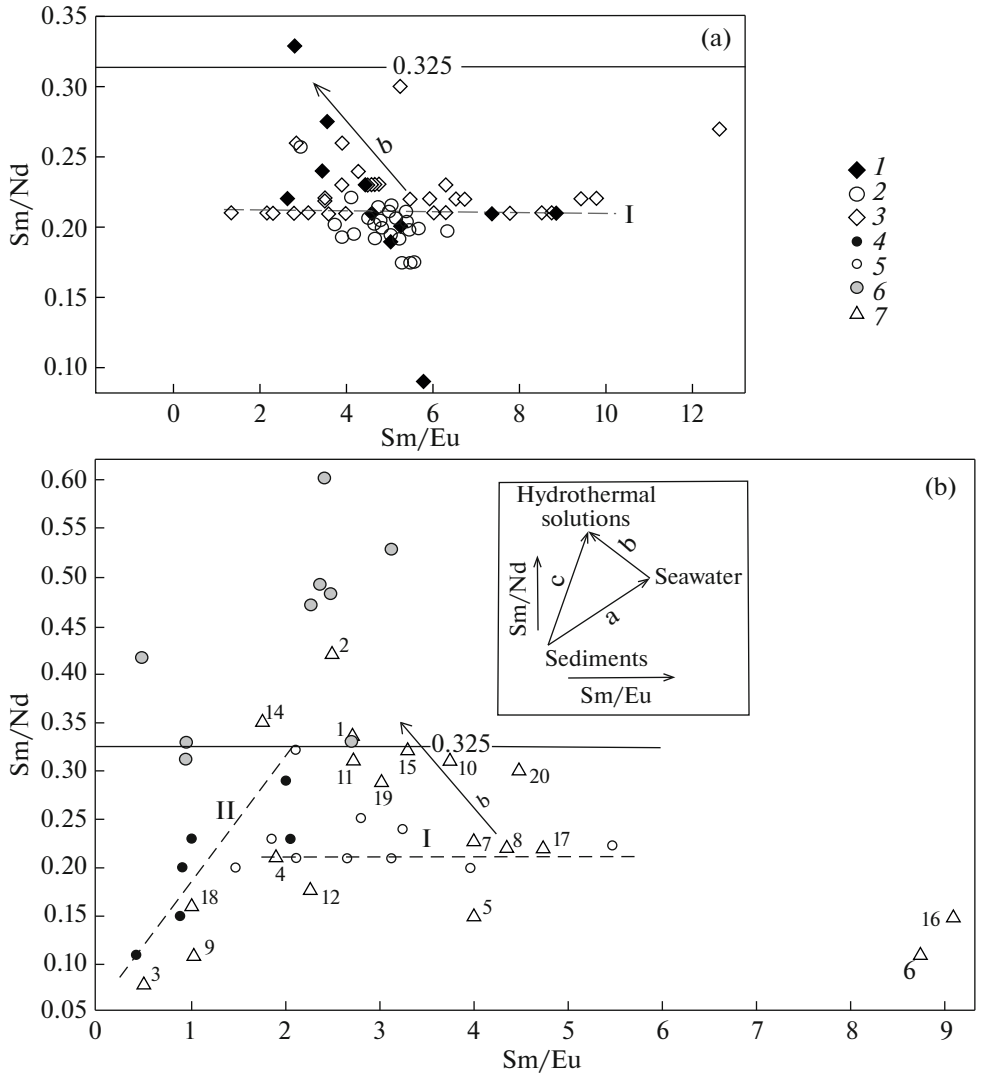

Fig. 10. Position of studied metamorphic and magmatic rocks of Sikhote-Alin in Sm/Nd–Sm/Eu diagram. Sedimentary (variably metamorphosed) rocks and ores (a) of Triassic chert formation: silicate–magnetite ores (*1*) and jaspers (*2*) of Shirokaya Pad area, manganese silicate rocks of Gornaya area (*3*). Magmatic rocks of (b) Vladimiro–Aleksandrovsky massif (*4*), Sergeevsky (*5*) and Kalinovsky (*6*) complexes. Metamorphic rocks (b) of orebodies of Belogorskoe deposit (*7*). Point numbers correspond to ordinal numbers of analyses in Table 1. Isoline 0.325 constrains maximum possible Sm/Nd ratio in magmatic rocks of Sergeevsky Complex and Vladimiro–Aleksandrovsky massif. In Figs. 10b (see inset) and 10a, arrows schematically show averaged vectors (a, b, c) of compositional changes of rocks and their protoliths (sediments with Sm/Nd and Sm/Eu characteristics of rocks of Vladimiro–Aleksandrovsky massif) owing to interaction with seawater and hydrothermal solutions.

Belogorskoe deposit (4, 12) from trend II to trend I (Fig. 10b).

Thus, we may suggest that a shift of data points of the Belogorskoe deposit from trend II to trend I along vector a or their alignment to trend I (Fig. 10) are caused by the different extent of seawater influence on the products of exogenic decomposition of gabbroids. This process is peculiar in approaching the Sm/Nd value to that of seawater (0.21), which, according to literature data on the ancient carbonate rocks was almost constant for a long-term geological history [12, 21]. Close values were typical of Triassic (Fig. 10a) during formation of protoliths (sediments) of the garnet and garnet–magnetite rocks of the Belogorskoe deposit.

The deviation of data points of Triassic jaspers and metamorphosed metalliferous sediments from trend I (Fig. 10a) is caused by a change of Sm/Nd and Sm/Eu ratios due to the influence of the mobile fluid phase during contact metamorphism. Similarly, data points of samples of the Belogorskoe deposit also plot beyond trends I and II and correspond to the hydrothermal alteration products of metamorphic rocks, in which the Sm/Nd and Sm/Eu initial (gabbroid) ratios were preliminarily (in terrigenous sediments) altered under the influence of seawater. As mentioned above, their

REE patterns retained negative Eu and positive Gd anomalies (Fig. 4b), which are typical of chemogenic and biogenic deposits of the Triassic chert formation of Sikhote-Alin. With increasing degree of hydrothermal alteration of these rocks in the Belogorskoe deposit (patterns 1, 11, 19), their REE patterns become significantly simplified and flattened, but a weak negative Eu anomaly is preserved (Fig. 4a).

Thus, a shift of data points from trend I along vector b (see inset to Fig. 10a) and flattening and smoothing of some REE patterns (Figs. 9a–9d) are the general features of hydrothermally altered samples of the Belogorskoe deposit, jaspers, manganese silicate rocks, and silicate–magnetite ores of the Triassic chert formation of Sikhote-Alin. These rocks and ores, just like the Belogorskoe deposit, are localized in the contact haloes of granitoid massifs, in particular, of the Vladimirsky granitoid massif, one of the exposures of which is the Shirokaya Pad massif. In general, comparison of Figs. 10b and 10a shows that the distributions of data points of the rocks of the Belogorskoe deposit and Triassic jaspers, manganese silicate rocks, and silicate–magnetite ores are similar, with some exceptions. In both cases, they are caused by the influence of seawater on the primary sediments and hydrothermal solutions on their metamorphosed analogues. The exceptions are the absence of data points of jaspers and metamorphosed Triassic metalliferous sediments in trend II due to the chemogenic–biogenic nature of their protoliths and relatively insignificant number of data points of the Belogorskoe deposit in trend I. The last fact is related to the different (not always extreme) degree of change in the initial Sm/Nd ratio in the protoliths of rocks (terrigenous sediments) of the Belogorskoe deposit under the influence of seawater and much wider manifestation of hydrothermal processes.

The peculiarities of the Belogorskoe orebodies indicate that they were formed under conditions of high temperature contact metamorphism of sediments and subsequent hydrothermal alterations with local redistribution of matter. Thus, they contain the products of two phases: metamorphic (garnet and magnetite–garnet rocks) and postmagmatic hydrothermal (morphologically and mineralogically diverse products of hydrothermal transformation of garnet and magnetite–garnet rocks). The contact metamorphism temperature was ~550°C at a lithostatic pressure of ~1.5 kbar, which approximately corresponds to the boundary of the amphibole–hornfels and epidote–amphibolite facies of contact and regional metamorphism, respectively (according to the classification by N.L. Dobretsov et al.) [8]. These conditions are consistent with the geological position of the Belogorskoe deposit (at the contact with the Vladimirsky granitoid massif) and previously obtained temperature values (~550°C) for the clinopyroxene–bustamite association of the Skal'naya orebody. They agree also with position of data points of the Ni–Co minerals in the diagram (Fig. 11), which indicates temperature ≥500°C. Minerals of metamorphic stage (Table 5) are attributed to a single mineral association (in a broad understanding of this term).

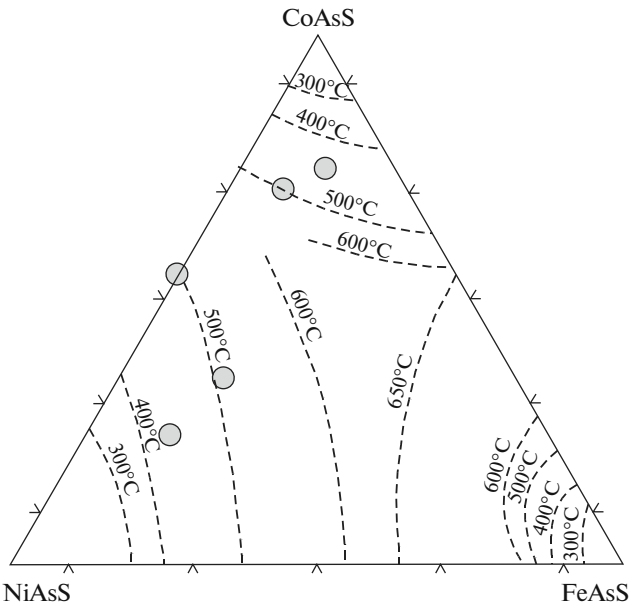

Fig. 11. Position of data points of cobaltite and gersdorffite of Belogorskoe deposit in diagram FeAsS–CoAsS–NiAsS. Isotherms after Klemm [32].

The hydrothermal stage related to postmagmatic hydrothermal activity [9] consisted of two phases. The earliest and highest temperature products of hydrothermal alteration are areas of diverse shape, which consists of manganactinolite or manganactinolite and rhodonite with inclusions of bismuth and molybdenum minerals (Table 5) and formed at 350–415°C. The main result of hydrothermal alteration of the second phase was the formation of numerous calcite veinlets, blocks of magnetite composition, and pockets mainly of coarse-crystalline calcite and, to a lesser extent, fluorite and sphalerite in the most reworked areas. The temperature (and, likely, the low temperature limit) of the formation of such pockets, judging from the presence of native bismuth, was ~270°C or slightly lower. The phases of the hydrothermal stage and corresponding assemblages of rock-forming and accessory minerals (Table 5) were distinguished conditionally, since hydrothermal process likely proceeded uninterruptedly with a gradual temperature decrease.

The main feature of hydrothermal alteration of metamorphic rocks is the decomposition of andradite, pyroxene, F-bearing, and other early minerals, and the release of Fe, Ca, Si, Mn, Sn (from andradite), Zn (from pyroxene), and some other elements. Fe and Sn were almost completely fixed in situ as magnetite and cassiterite. Ca, Mn, Zn, and other released elements (Au, Ag, Bi, Pb, Mo, and W) locally migrated and pre-

Table 5. Stages, phases, and mineral associations of main orebodies of Belogorskoe deposit

Stages	Phases	Mineral and morphological types of separations	Mineral associations
Metamorphic	–	Bodies of garnet as well as banded garnet–magnetite rocks	Andradite*, magnetite*, clinopyroxene**, bustamite**, vesuvian**, datolite**; cuspidine**; apatite, zircon, baddeleyite, thorianite; thorite, ilmenite–pyrophanite, rutile; barite, wolframite; scheelite, cobaltite–gersdorffite, loellingite, arsenopyrite, native gold without admixtures, gold–silver solid solution, native platinum; platinum and palladium compounds, and other noble metal minerals
Hydrothermal (postmagmatic)	Early (medium-temperature)	Actinolite–rhodonite pockets of irregular shape up to a few cm in diameter	Rhodonite*, actinolite*, calcite**, andradite**, molybdenite, Bi_2Te, Bi_4Te, Bi_5Te, and Bi_6Te
	Late (low-temperature)	Small later calcite pockets in garnet and garnet–magnetite rocks; systems of calcite (with relict garnet) veinlets cutting whole volume of garnet and magnetite–garnet rocks; large blocks of massive magnetite in most altered areas of garnet and garnet–magnetite rocks; pockets of coarse-crystalline calcite up to 1 m across and greater in magnetite blocks	Magnetite*, calcite*, fluorite*, sphalerite*, andradite**, actinolite**, rhodonite**, cassiterite, molybdenite, scheelite–povellite, native Bi, bismuthine, joseite A, cosalite, gladite, jonassonite, galenobismutite, Bi_3Te_2, (Bi,Ag)(S,Te), Bi_3S_4, (Pb,Ag)BiS_2, Ag-tetrahedrite, polybasite, cinnabar, coloradoite, $Ag_4Sb_2S_3$ compound (?), ullmannite, stibnite, native Sb, native gold without admixtures, copper gold, native platinum, and other minerals of noble metals
Exogenic		Euhedral and xenomorphic minerals in rocks and cavities of exogenic leaching	Preisingerite, bastnaesite, bismite, bismutite, dobreite, zavaritskite, ilsemanite, lafossaite, massicot, and others

* major minerals, ** subordinate minerals, others are accessory minerals.

cipitated in different mineral forms within calcite (with fluorite, relict andradite, and other minerals) veinlets crosscutting the whole volume of orebodies, as well as in mangano-actinolite–rhodonite segregations and pockets of coarse-crystalline calcite [9]. The formation of the latter within magnetite blocks compensated the deficiency of volume formed during replacement of garnet by magnetite with removal of Si. A decisive role in the formation of pockets of coarse-crystalline calcite was played by volatiles (CO_2, F_2, and S_2) that bound Ca, Mn, Zn, Bi, Ag, Pb, and Mo in the carbonate, fluoride, or sulfide mineral forms. The precipitation of calcite (and associated accessory minerals) was repeatedly altered by precipitation of fluorite (which makes up large monomineralic areas in calcite) or sphalerite (which forms short veins along cleavage planes in calcite and fluorite), accessory sulfides, and oxides, which indicates mutual and significant changes in CO_2, F_2, S_2, and O_2 activity in hydrothermal solutions.

The mineral assemblages of the hydrothermal stage formed mainly owing to the release, local redistribution, and precipitation (under favorable conditions) in different mineral forms of chemical elements present earlier in orebodies: both those that make up the minerals proper (Ca, Fe) and those that were dispersed in other minerals (Mn, Sn, Zn, Bi, Pb, Ag, Au, Mo, and W). The main precipitators of these elements in rocks of the second phase of the hydrothermal process were volatile components, such as CO_2, F_2, and S_2.

The orebodies of the Belogorskoe deposit contain rare and weakly studied minerals and mineral varieties. The latter include unusually Th-rich zircon, baddeleyite, gudmundite, a large group of bismuth compounds, including Bi_2Te, (Ag,Pb)BiS_2, as well as coloradoite, lafossaite, sanbornite, perovskite, and the

compound $InPO_4$. There are also a large group of rare and compositionally unusual noble metal compounds: copper gold, platinum gold, jonassonite, disordered solid solutions of Cu, Ag, and Au (based on Au), intermetallides of Pt and Pd, Pt and Ag, and other rare minerals and mineral varieties.

CONCLUSIONS

New materials were obtained in support of the concept previously substantiated by geological, geochemical, and isotope data that the orebodies of the Belogorskoe deposit are the Triassic erosion products of the laterite weathering crust after gabbroid, which were metamorphosed and partially regenerated in the Late Cretaceous–Paleogene.

Sources of metals of the Belogorskoe deposit were the exogenic decomposition products of rocks that are isotopically and geochemically close to the gabbroids of the Vladimiro–Aleksandrovsky massif. This conclusion is confirmed by the enrichment of orebodies in elements typical of ultramafic rocks, Fe and Mn, and by the presence of Au–Ag–Pd–Pt, Ni-Co, and Bi mineralization.

The orebodies of the Belogorskoe deposit consist of rocks, the primary (gabbroid) REE distribution in which was variably modified through the interaction of sediments (protoliths) with seawater and their metamorphosed analogues with hydrothermal solutions.

FUNDING

This study was supported by ongoing institutional funding. No additional grants to carry out or direct this particular research were obtained.

CONFLICT OF INTEREST

The authors of this work declare that they have no conflicts of interest.

REFERENCES

1. V. N. Anfilogov, A. A. Krasnobaev, and V. M. Ryzhkov, "Ancient age of zircons and problems of genesis of dunites from gabbro–gyperbasite complexes of orogenic areas and platform massifs of central type," Litosfera **18** (5), 706–717 (2018).
2. N. S. Blagodareva, I. N. Govorov, E. A. Lagovskaya, and S. P. Slavkina, "Data on mineralogy of the Sadovyi lead–zinc deposit," *Problems of Mineralogy, Magmatism, and Ore Genesis of the Far East* (DVNTs AN SSSR, Vladivostok, 1974), pp. 79–92 [in Russian].
3. G. P. Volarovich, "Geology of the Ol'ga iron ore deposits and their assessment," Zap. Vsesoyuz. Mineral. O-va **69** (1), 121–134 (1940).
4. *Geodynamics, Magmatism, and Metallogeny of East Russia*, Ed. by A. I. Khanchuk (Dal'nauka. Vladivostok, 2006) [in Russian].
5. Yu. D. Gritsenko and E. M. Spiridonov, "Sulfoarsenides and sulfoantimonides of nickel, cobalt, iron, and krutovite from metamorphogenic–hydrothermal carbonate veins of the Norilsk ore field," New Data on Minerals **41**, 46–55 (2006).
6. T. Ya. Gulyaeva and S. A. Shcheka, "Microinhomogeneities of scarce varieties of magnetite and their genetic significance," *Minerals as Indicators of Petrogenesis* (Vladivostok, 1980), pp. 62–68 [in Russian].
7. T. Ya. Gulyaeva and S. A. Shcheka, "On trace Zn–Mg-manganese variety of magnetite," Dokl. Akad. Nauk SSSR **267** (6), 1448–1453 (1982).
8. N. L. Dobretsov, V. V. Reverdatto, V. S. Sobolev, and N. L. Dobretsov, *Metamorphic Facies* (Nedra, Moscow, 1970) [in Russian].
9. V. T. Kazachenko, E. V. Perevoznikova, and S. N. Lavrik, Mineralogy and genesis of the Belogorsk skarn–magnetite deposit (Primorye)," Tikhookean. Geol. **30** (6), 67–83 (2011).
10. V. T. Kazachenko and E. V. Perevoznikova, "Isotopic (Sm–Nd) and geochemical (Nb/Y–Zr/Y) systematics of the Sikhote-Alin basic-hyperbasic complexes," Geochem. Int. **61** (4), 324–347 (2023).
11. I. V. Kemkin, *Extended Abstract of Doctoral Dissertation in Geology and Mineralogy* (Vladivostok, 2003) [in Russian].
12. M. T. Krupenin, A. B. Kuznetsov, and G. V. Konstantinova, "Comparative Sr-Nd-systematics of carbonate rocks in the typical Lower Riphean magnetite deposits of the South Uralian Province," Ezhegodnik-2014. Tr. IGG UrO RAN **162**, 100–106 (2015).
13. G. M. Lobanova, "Conditions of occurrences of cuspidine and monticellite skarns in the deposits of the Southern Primorye," Zap. Vsesoyuz. Mineral. O-va **89** (5), 523–541 (1960).
14. V. M. Okrugin, N. A. Malik, E. Yu. Plutakhina, M. A. Nazarova, V. V. Kozlov, S. V. Moskaleva, and M. V. Chubarov, "New data on exhalations and sublimates of the Avacha volcano (2014–2015)," *Conference Dedicated to the Volcanologist's Day in IViS DVO RAN "Volcanism and Related Processes,"* (2016), pp. 400–405 [in Russian].
15. A. I. Ponomarenko, "Rhodonite–spessartine rocks of the Anabar massif," Dokl. Akad. Nauk SSSR **212** (6), 1426–1429 (1973).
16. E. A. Radkevich, G. M. Lobanova, I. N. Tomson, Yu. S. Borodaev, N. N. Mozgova, L. N. Khetchikov, A. I. Aleksandrov, V. P. Solyanikov, and S. I. Smirnov, *Geology of the Lead–Zinc Deposits of Primorye* (AN SSSR, Moscow, 1960), **Vol. 1** [in Russian].
17. F. I. Rostovskii, *Extended Abstract of Candidate's Dissertation in Geology and Mineralogy* (Vladivostok, 1975).
18. V. G. Sakhno, F. I. Rostovskii, and A. A. Alenicheva, "U–Pb isotope dating of igneous complexes from the Milogradovo gold–silver deposit (Southern Primor'e)," Dokl. Erth Sci. **433** (1), 879–886 (2010).
19. L. F. Simanenko and V. V. Ratkin, *Partizanskoe Skarn–Basemetal Deposit: Geology, Mineralogy, and Genesis (Taukha Metallogenic zone, Sikhote-Alin')* (Nauka, Moscow, 2008) [in Russian].

20. V. I. Smol'yaninova and S. E. Borisovskiy, "Pyrophanite in manganese ores of the Prozrachnoe deposit (Gornyi Altai)," Izv. Akad. Nauk SSSR. Ser. Geol., No 9, pp. 131–136 (1984).

21. G. Faure, *Principles of Isotope Geology* (Wiley, New York, 1986).

22. L. N. Khetchikov, "Geological structure and mineralogy of the Pervyi Sovetskii rudnik (Tetyukhe) deposit," *Proceedings of Geology, Mineral Resources, and Mineralogy of the Southern Far East* (AN SSSR, Moscow–Leningrad, 1960), pp. 53–187 [in Russian].

23. F. Bea, "Residence of REE, Y, Th and U in granites and crustal protoliths; implications for the chemistry of crustal melts," J. Petrol. **37** (3), 521–552 (1996).

24. B. Charoy and P. J. Pollard, "Albite-rich, silica-depleted metasomatic rocks at Emuford, Northeast Queensland: mineralogical, geochemical, and fluid inclusion constraints on hydrothermal evolution and tin mineralization," Econ. Geol. **84**, 1850–1874 (1989).

25. A. J. Criddle and C. J. Stanley, *Quantitative Data File for Ore Minerals,* Third Edition (Chapman & Hall, London, 1993).

26. S. Dasgupta, M. Fukuoka, and S. Roy, "Hematite–pyrophanite intergrowth in gondite, Chikla Area, Sausar Group, India," Mintr. Mag **48**, 558–560 (1984).

27. N. M. Evensen, P. J. Hamilton, and R. K. O' Nions, "Rare earth abundances in chondritic meteorites," Geochim. Cosmochim. Acta **42**, 1199–1212 (1978).

28. G. Faure, *Principles of Isotope Geology* (John Wiley & Sons, New York, 1986).

29. H. J. Forster, "Composition and origin of intermediate solid solutions in the system thorite–xenotime–zircon–coffinite," Lithos **88**, 35–55 (2006).

30. B. M. Jahn, G. A. Valui, N. N. Kruk, V. G. Gonevchuk, M. Usuki, and J. T. J. Wu, "Emplacement ages, geochemical and Sr-Nd-Hf isotopic characterization of Mesozoic to Early Cenozoic granitoids of the Sikhote-Alin orogenic belt, Russian Far East: crustal growth and regional tectonic evolution," J. Asian Earth Sci. **111**, 872–918 (2015).

31. J. L. Jambor, "New lead sulfantimonides from Madoc, Ontario, Part I," Can. Mineral. **9**, 7–24 (1967).

32. D. D. Klemm, "Synthesen und analysen in den dreiecks diagrammen FeAsS–CoAsS–NiAsS und FeS_2–CoS_2–NiS_2," Neues Jahrb. Mineral. Abh. **103**, 205–255 (1965).

33. D. E. Lee, "Occurrence of pyrophanite in Japan," Am. Mineral. **40**, 32–40 (1955).

34. M. T. McCulloch and J. A. Gamble, "Geochemical and geodynamical constraints on subduction zone magmatism," Earth Planet. Sci. Lett. **102**, 358–374 (1991).

35. W. F. McDonough, S. Sun, A. E. Ringwood, E. Jagoutz, A. W. Hofmann, "K, Rb and Cs in the Earth and Moon and the evolution of the Earth's mantle," Geochim. Cosmochim. Acta, **56** (3), 1001–1012 (1992).

36. Y. Moelo, E. Macovicky, N. N. Mozgova, J. Jambor, N. Cook, A. Pring, W. H. Paar, E. Nickel, S. Graeser, S. Karup-Moller, T. Balic-Zunic, W. G. Mumme, F. Vurro, D. Topa, L. Bindi, K. Bente, and M. Shimizu, "Sulfosalt systematics: a review. Report of the Sulfosalt Sub-Committee of the IMA Commission on Ore Mineralogy," Eur. J. Mineral. **20**, 7–46 (2008).

37. A. Mucke and C. Okujeni, "Geological and ore microscopic evidence on the epigenetic origin of the manganese occurrences in northern Nigeria," J. Afr. Earth Sci. **2** (3), 209–225 (1984).

38. H. Palme and H. St. C. O' Neill, "The mantle and core," Treatise Geochem. **2**, 1–38 (2003).

39. A. C. Roberts, K. E. Venance, T. M. Seward, J. D. Grice, and W. H. Paar, "Lafossaite: a new mineral from the La Fossa Crater, Vulcano, Italy," Mineral. Record, No. **37**, 165–168 (2006).

40. C. Sivaprakash, "Mineralogy of manganese deposits of Kodura Garbham, Andra Pradesh, India," Econ. Geol. **75** (7), 1083–1104 (1980).

41. S. S. Sun and W. F. McDonough, "Chemical and isotopic systematics of oceanic basalts: implications for mantle composition and processes," *Magmatism in the Ocean Basins,* Ed. by A. D. Saunders and M. J. Norry, Geol. Soc. London, Spec. Publ. **42**, 313–345 (1989).

42. R. E. Walstrom and J. F. Leising, "Barium Minerals of the Sanbornite deposits, Fresno County, California," Axis **1** (8), 1–18 (2005).

43. D. A. Wood, J. L. Joron, M. Treuil, M. Norry, and J. Tarney, "Elemenntal and Sr isotope variations in basic from Iceland and surrounding ocean floor," Contrib. Mineral. Petrol. **70**, 319–339 (1979).

44. V. Zacek, R. Skodà, and P. Sulovsky, "U-Th-rich zircon, thorite and allanite-(Ce) as main carriers of radioactivity in the highly radioactive ultrapotassic melasyenite porphyry from the Sumava Mts., Moldanubian Zone, Czech Republic," J. Geosci. **54**, 343–354 (2009).

Recommended for publishing by A.I. Khanchuk

Translated by M. Bogina